

# Investigation of the relationship between CPT cone resistance and friction angle for a range of granular soils

Yishan Tian<sup>1,2</sup>, Barry Lehane<sup>1#</sup>

<sup>1</sup>Department of Civil, Environmental and Mining Engineering, University of Western Australia,  
 35 Stirling Highway, Crawley, Perth, Western Australia

<sup>2</sup>Fugro Belgium, EUAF GeoConsulting Marine Geotech, Rue du Bosquet 9, Louvain-la-Neuve, Belgium

#Corresponding author: barry.lehane@uwa.edu.au

## ABSTRACT

This paper presents an investigation of the effects of the properties of reconstituted granular soils on the relationship between CPT cone resistance ( $q_c$ ) and friction angle. The results from a large number of calibration chamber tests conducted at a number of stress levels involving soils with varying shapes, compressibility and mineralogy are presented. The paper also provides data recorded in a parallel series of investigations into the mechanical properties of the granular soils employed in the chamber tests. It is shown that the nature of granular deposits has a strong influence on the relationship between  $q_c$  and relative density, and that there is a near linear relationship between the cone resistance and the critical state friction angle for sands reconstituted at a given density and stress level.

**Keywords:** Cone penetration test; granular soil; friction angle.

## 1. Introduction

The Cone Penetration Test (CPT) is a very popular in-situ testing method that assists site characterization and provides data for a direct application in design. The dependence of the cone resistance ( $q_c$ ) on the mechanical properties of granular soils is well known and this dependence is often used to assess their relative density ( $D_r$ ). Typical proposed correlations relating  $q_c$  and  $D_r$  for coarse-grained soils are of following format:

$$D_r = C_1 \ln[q_{c1N}/C_2] \quad (1a)$$

$$q_{c1N} = (q_c/p_{atm})/(\sigma'/p_{atm})^n \quad (1b)$$

where  $q_{c1N}$  = stress normalized cone resistance;  $C_1$  and  $C_2$  are empirical constants,  $p_{atm}$  = atmospheric pressure (100 kPa),  $n$  = stress level exponent and  $\sigma'$  = effective stress at the level of the cone tip.

It is also well known that the peak friction angle of a sand varies with the relative density and stress level. This dependence has given rise to correlations such as those of Robertson and Campanella (1983) relating peak friction angles ( $\phi'_p$ ) at a nominated confining stress with cone resistance and relative density. The compressibility and mineralogy of the sand has been shown by a number of workers to affect the  $q_c$ - $D_r$ - $\phi'_p$  correlation.

The effect of particle shape on friction angle of granular materials has been investigated by characterizing the shape using quantitative measurements such as sphericity ( $S$ ), roundness ( $R$ ) and regularity ( $\rho$ ). Miura et al. (1998) showed that  $\phi'_p$  increases with decreasing regularity while Santamarina and Cho (2004) shows higher particle irregularity results in an increase in both peak and ultimate friction angles ( $\phi'_p$  and  $\phi'_{cv}$ ). Liu and Lehane (2012) proposed the following linear relationships between  $\phi'_{cv}$  (in degrees) and both  $R$  and  $\rho$ :

$$\phi'_{cv} = 41 - 16.6R \quad (2a)$$

$$\phi'_{cv} = 43 - 18\rho \quad (2b)$$

This paper reports results from a systematic laboratory investigation using six different granular soils with various particle shapes and mineralogy. Relationships between cone resistance, relative density, friction angle, particle shape and particle mineralogy are examined with the aim of evaluating the suitability of existing relationships and extending their applicability to a wider range of granular materials.

## 2. Granular materials investigated

Details of the materials investigated in this study are

**Table 1.** Index properties of materials used in this study

Sand type	Mineralogy	Specific gravity	Gradation		Particle shape		
		$G_s$	$d_{50}$	$C_u$	$R$	$S$	$\rho$
UWA sand	Siliceous	2.67	0.15	1.4	0.68	0.62	0.66
LP sand	Calcareous	2.76	0.34	2	0.3	0.3	0.3
GBS	Siliceous	2.49	0.2	1.62	1	1	1
GBM	Siliceous	1.08	0.75	1.54	1	1	1
GBL	Siliceous	0.53	0.9	1.46	1	1	1
SS	Steel	7.85	0.23	1.65	1	1	1

\*The low apparent  $G_s$  values of GBM and GBL arise due to application of the standard testing technique to hollow glass particles

summarized in Table 1. The UWA sand is a fine silica sand sourced commercially and has been tested extensively over the past two decades at the University of Western Australia (UWA). Three types of spherical uniform Ballotoni glass beads were employed with mean effective particles sizes ( $d_{50}$ ) of 0.2mm, 0.75mm and 0.9mm, referred to respectively as GBS, GBM and GBL. Spherical stainless steel shots (SS) with  $d_{50}=0.23$ mm were investigated to compare the effect of mineralogy with the similarly sized GBS material. An angular carbonate sand (LP), typically of beach sands found on the west coast of Australia, is also included to extend the scope of the study.

All materials investigated are uniformly graded with a uniformity coefficient ( $C_u$ ) of between 1.4 and 2. Oedometer tests indicated that the three sizes of spherical glass beads examined had a very low compressibility with a compression index ( $C_c$ ) of approximately 0.005 at 100kPa. This compares with the  $C_c$  values at the same stress level obtained for the standard silica (UWA) sand and LP carbonate sand of about 0.008 and 0.02 respectively. The steel shots had the lowest  $C_c$  with an approximate value of 0.004. Therefore all materials can be assumed to fall into the low compressibility category apart from the LP sand which has medium compressibility when compared with the data in Mesri and Vardhanabhuti (2009).

### 2.1. Direct-shear tests

A circular 72mm diameter shear box, developed in-house at UWA, was employed to test all materials. Liu and Lehane (2012), and others, show that the peak and ultimate friction angles of dry and saturated sands are identical. Therefore all materials were tested dry and sheared at a constant rate of 1mm/min. The relative density ( $D_r$ ) of all samples tested was held constant at approximately 0.65 and tests were conducted at normal stresses ( $\sigma'_v$ ) of 50kPa, 100kPa and 200kPa.

Typical results are shown in Fig.1 for the six materials at a normal stress of 50kPa. All samples develop a peak resistance at a displacement of about 1.5mm and ultimate conditions at a displacement of 4mm. Highest peak and ultimate friction coefficients ( $\tau/\sigma'_v$ ) are developed by the carbonate sand, consistent with its higher level of dilation. The steel shots showed

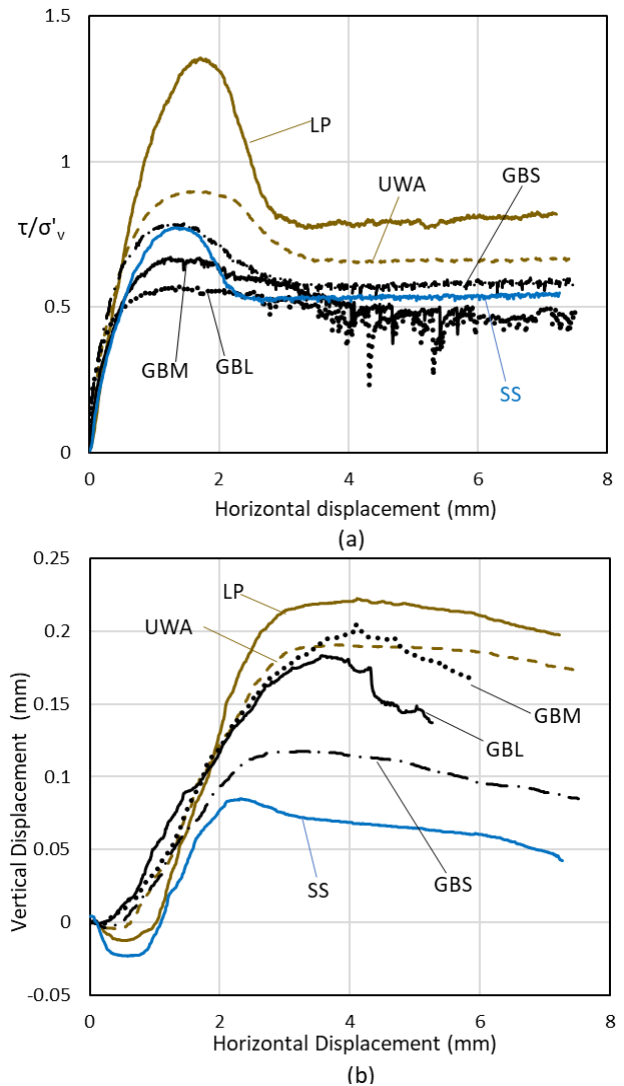


**Figure 1.** Typical shear-box test results on all material at  $D_r=65\%$

the lowest level of dilation but its peak friction was greater than that of GBM and GBL.

The peak friction angle  $\phi'_p$  recorded at  $\sigma'_v=50$ kPa and the mean ultimate friction, recorded at the three stress levels ( $\phi'_{cv}$ ) are summarized in Table 2. Data from other tests on glass particles reported by Liu and Lehane (2012), termed GB0 and GB1 are included in the table, where the GB0 is a round glass material and GB1 is a more angular glass with  $d_{50}$  of 0.12mm and 0.45mm.

**Table 2.** Measured Friction angle and inferred peak friction angle from  $q_c$  and  $\sigma'_v$ .

Sand type	$\phi'_p$ ( $^\circ$ )	$\phi'_{cv}$ ( $^\circ$ )	$q_c$		$\phi'_p$ (calculated from Empirical Relationships at $\sigma'_v=50$ kPa)	
	$\sigma'_v=50$ kPa		$\sigma'_v=50$ kPa	$\sigma'_v=75$ kPa	Robertson and Campanella (1983)	Jamiolkowski, Lo Presti and Manassero (2003)
UWA	42	32.4	8.1	11.2	42.8	42.0
GBS	38.2	30.2	6.1	8.6	41.6	41.0
GBM	33.9	27.4	4.4	6.6	40.3	40.0
GBL	31.9	26.0	4.1	5.4	39.3	38.5
LP	53.6	38.5	10.7	15	44.0	46.8
SS	37.3	26.8	-	-		
GB0	-	25.5	-	4.8		
GB1	-	32.5	-	13.1		

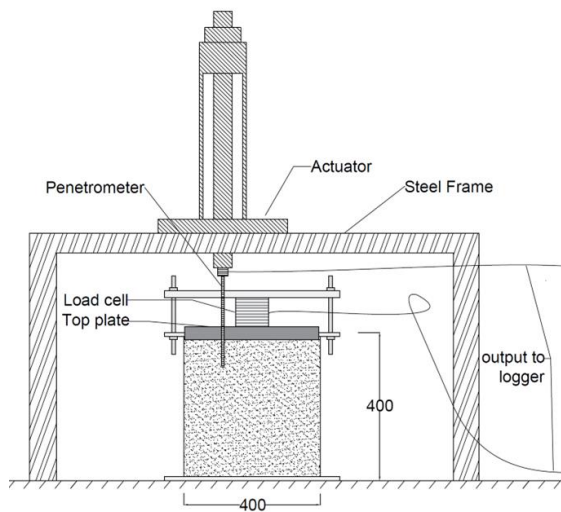


Figure 2. Schematic of the calibration chamber test.

## 2.2. Cone penetration test

Cone penetration tests were conducted on each reconstituted sample of each material in circular pressure (calibration) chambers, shown schematically in Fig. 2. All soil samples were prepared by dry pluviation using a constant drop height to achieve sample uniformity. A rigid horizontal bar is positioned above the top plate of the chamber and is held in place by a pair of threaded rods. The vertical effective stress is controlled by tightening or untightening of locking nuts on top of the horizontal bar, and is monitored by a load cell placed between the bar and top plate. The top plate has circular openings to allow for penetrometer access to the sample. The overburden stress and cone resistance are recorded while the cone is driven into the sample at a constant speed by the actuator located on the steel frame. A 6mm penetrometer was used for UWA sand, LP sand, GBS and SS and a 16mm penetrometer was used for the GBM and GBL soils to maximise the ratio of the cone diameter ( $d_c$ ) to mean effective particle size ( $d_{50}$ ).

Typical calibration chamber test results are presented in Fig. 3 for GBS with a relative density ( $D_r$ ) of 0.65

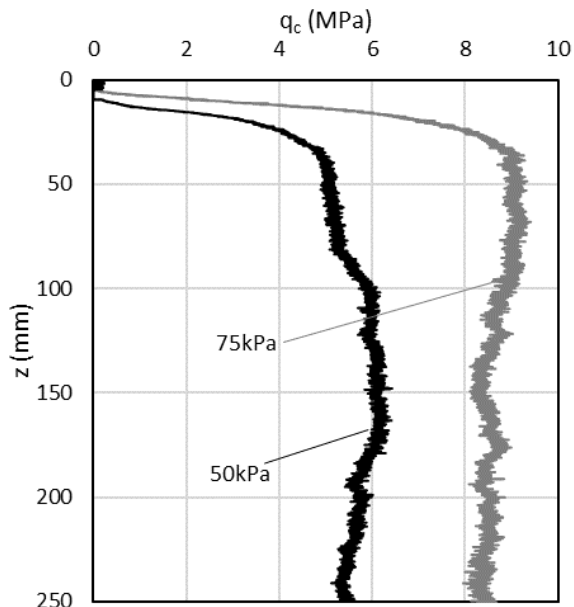
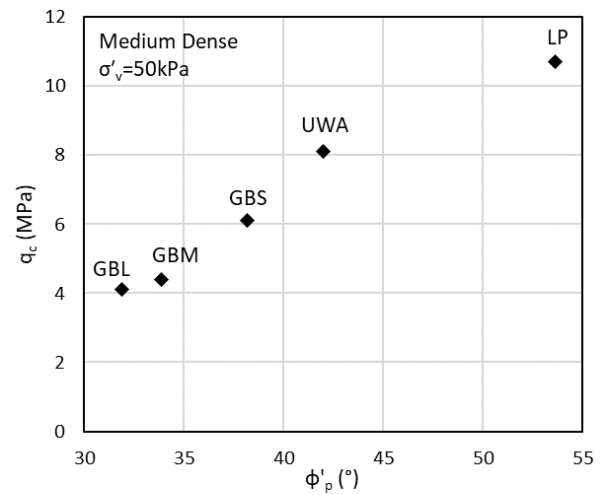
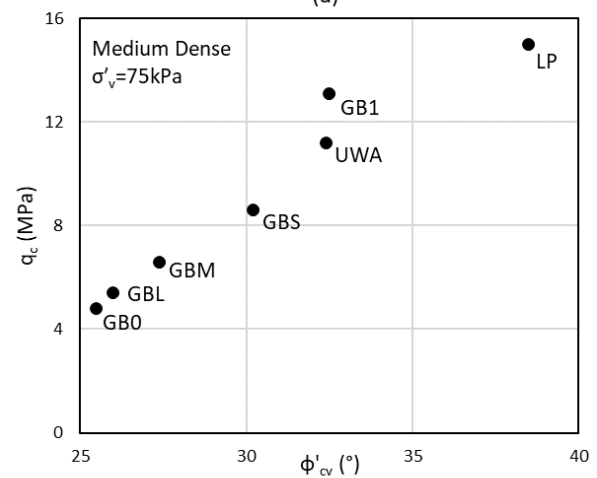


Figure 3.  $q_c$  profile measured in medium dense GBS



(a)



(b)

Figure 4. Relationship between  $q_c$  of materials tested and (a)  $\phi'_p$ , (b)  $\phi'_{cv}$

(i.e. the same as used in the shear box tests) and at applied vertical stresses of 50kPa and 75kPa. The chamber side wall is coated with Teflon spray to reduce side friction. It can be seen that the reduction in  $q_c$  is very limited with depth which reflects minimum friction loss and uniform stress conditions. The steady state  $q_c$  values, recorded below a depth of 100mm, for all materials are presented in Table 2. Despite the low oedometric compressibility of the glass ballotini, distinctive ‘popping’ sounds were heard during cone penetration indicating particle fracture under the shear applied during penetration. No obvious noise was heard during penetration in LP carbonate sand which has a relatively high oedometric compressibility.

## 3. Results and Discussion

### 3.1. Cone resistance relationship with friction angle

The  $q_c$  values measured in samples with  $D_r \sim 0.65$  under a vertical stress of 50kPa are plotted on Fig. 4(a) against the peak friction angle from shear-box tests recorded at the same  $D_r$  with  $\sigma'_v = 50$  kPa. It can be clearly seen that  $q_c$  increases systematically with  $\phi'_p$ .

Robertson and Campanella (1983) proposed Eq. (3) for peak friction angles (presumably at low to moderate

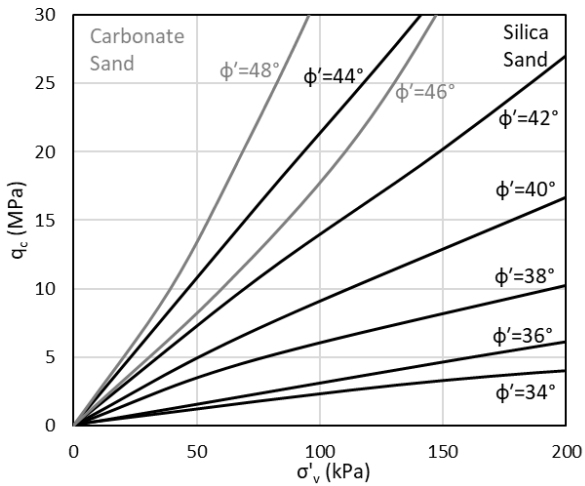


**Figure 5.**  $q_c$ - $\sigma'_v$  relationships by Jamiolkowski, Lo Presti and Manassero (2003)

stress levels) while Jamiolkowski, Lo Presti and Manassero (2003) suggested the  $\phi'_p$  dependent  $q_c$ - $\sigma'_v$  relationships for silica and carbonate sands shown in Fig. 5.

$$\tan\phi'_p = \frac{1}{3} \left[ \log\left(\frac{q_c}{\sigma'_v}\right) + 0.6 \right] \quad (3)$$

The values of  $\phi'_p$  determined using Eq. (3) and Fig. 5 are compared in Table 2 with measured values at  $\sigma'_v = 50$  kPa. Both sets of equations provide good predictions for UWA, GBS and GBM sands, over-predicting  $\phi'_p$  by an average of about 10%. Greatest over-predictions were seen for the large glass ballotini (GBL) which is partly due to its low ultimate friction angle compared with typical sands. Both relationships under-predict  $\phi'_p$  values of LP calcareous sand by 15 to 20%.

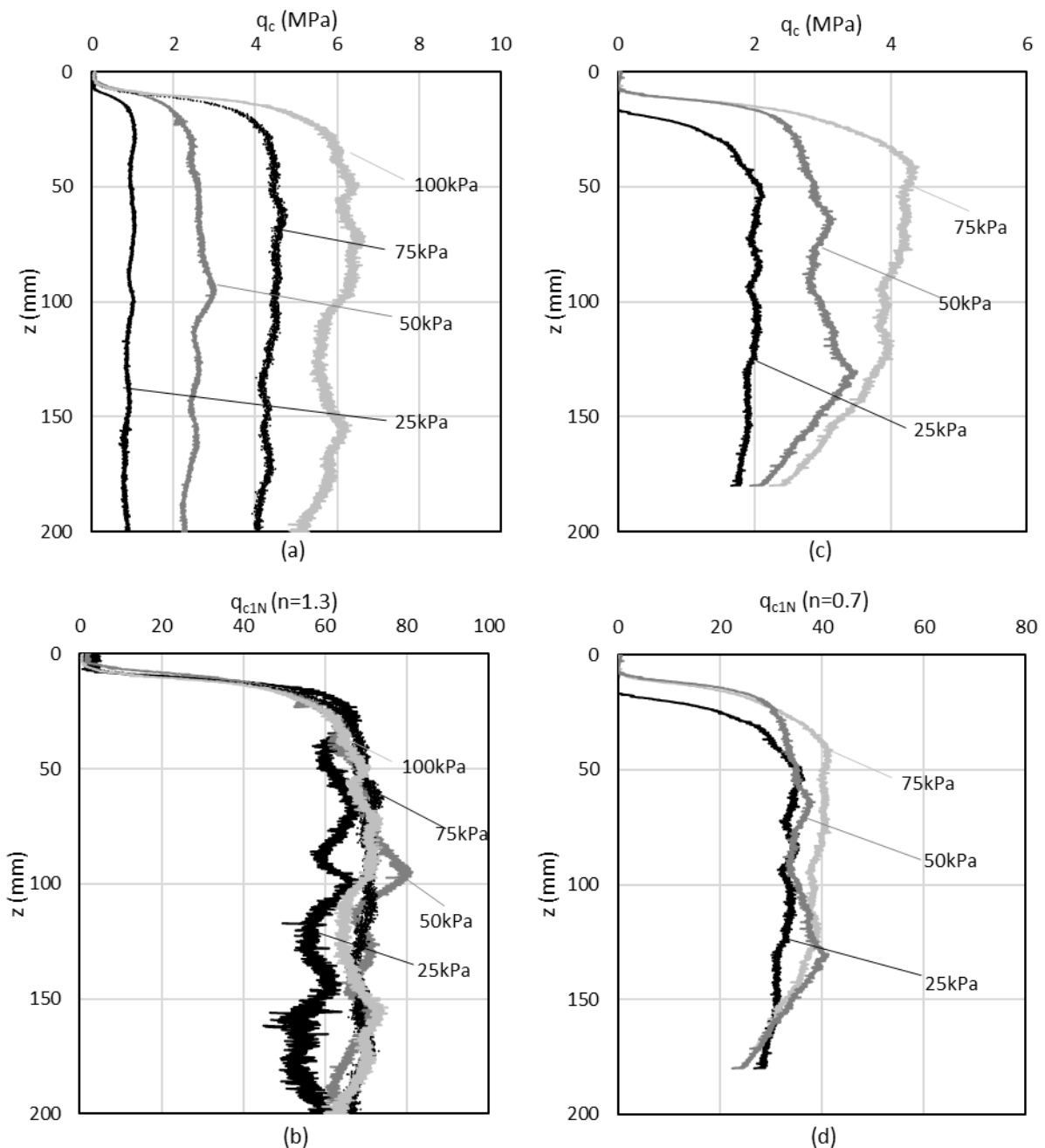


**Figure 6.** CPT result in form of (a)  $q_c$  (b)  $q_{c1N}$  in loose GBS and (c)  $q_c$  (d)  $q_{c1N}$  in loose SS

Figure 4(b) plots the variation of  $q_c$  with  $\phi'_{cv}$  for the six materials listed in Table 1 and the two additional glass materials (GB0 and GB1, mentioned previously). Results are shown for an applied vertical stress in the chamber of 75 kPa. It can be seen that, as for the peak friction angle,  $q_c$  increases in a near linear way with  $\phi'_{cv}$ . This result is interesting given the range of particle characteristics and mineralogy considered and suggests that relationships between  $q_c$  and  $D_r$  (such as given in Eq. (1) should also include a  $\phi'_{cv}$  term. Such an approach is feasible given that  $\phi'_{cv}$  can generally be estimated relatively accurately from published trends with a knowledge of the particle shape (e.g. Eq. 2), mineralogy and uniformity coefficient. Alternatively the value of  $\phi'_{cv}$  can be assumed equal to the measured angle of repose of a dry sand heap.

By comparing published results of CPTs in various types of carbonate sand and silica sand, Giretti et al. (2018) conclude that the compressibility of carbonate sands causes reduced cone resistance compared with silica sands. A similar conclusion was drawn by Ciantia et al. (2016) from discrete element numerical modelling. However, as seen on Fig. 4, this inference is not in line with the results of this study, which shows that lowest cone resistances are obtained in the soils with smallest  $\phi'_{cv}$  values, irrespective of a soil's compressibility, shape, crushability and mineralogy.  $\phi'_{cv}$  appears to be the dominant controlling parameter affecting  $q_c$  in granular soils at a constant  $D_r$  and stress level. It is clear that further testing is required to isolate the effects of compressibility and friction angle on the cone resistance.

### 3.2. Stress exponent $n$

The stress exponent ' $n$ ' allows the effect of stress level on the cone resistance to be accommodated in the calculation of the normalized cone resistance,  $q_{c1N}$ , which varies with the soil relative density (see Eq. 1). The value of  $n$  of often assumed to be about  $0.7 \pm 0.1$  in sands (Lunne and Christoffersen 1983, Salgado and Prezzi 2007, Idriss and Boulanger 2008, Tian and Lehane 2022, Lehane et al. 2023). Salgado and Prezzi (2007) and Idriss and Boulanger (2008) suggest that  $n$  decreases with increasing  $D_r$ , while Bolton, Gui and Phillips (1993), Liao and Whiteman (1986), Strum (2019) assumed little dependence of  $n$  on  $D_r$ .

Figure 6 examines the most appropriate  $n$  value for very loose GBS and SS samples ( $D_r=0.15$ ), which were tested at either three or four different stress levels. The cone resistances are shown in Fig. 6(a) and Fig. 6(c) and the normalized cone resistances ( $q_{c1N}$ ) profiles are shown on Fig. 6(b) and Fig. 6(d). The value of  $n$  selected for both soils is that which gave a constant  $q_{c1N}$  with depth, as the relative density in the chambers was constant. It is evident that while the  $n$  value for the steel shots is in good agreement with that typically employed in sands, the best fit value for very loose GBS was 1.3 and almost double the standard value. Higher density GBS samples (see Fig. 3) indicated that an  $n$  value of 0.7 was suitable indicating that high  $n$  value for GBS shown on Fig. 6(a) is only applicable to very loose glass ballotini. Further research is required to better understand factors affecting the  $n$  values.

## 4. Conclusions

CPTs were performed in calibration chambers at UWA to study the effect of friction angle on the relationship between cone resistance ( $q_c$ ), stress level ( $\sigma'_v$  or  $p'$ ) and relative density ( $D_r$ ) of granular media. It was found that this relationship varied systematically with the ultimate friction angle ( $\phi'_{cv}$ ) of the material and that  $q_c$ - $D_r$ - $\sigma'_v$  expressions in common use should also incorporate  $\phi'_{cv}$ , to reflect its strong dependence on the particular  $q_c$ - $D_r$ - $\sigma'_v$  relationship for a given soil. Such an approach is feasible given that  $\phi'_{cv}$  can generally be estimated relatively accurately from published trends or by measuring the angle of repose.

The research also highlighted some of the differences between materials of the density dependence of the stress level exponent,  $n$ , used to calculate normalized cone resistance.

## Acknowledgements

The authors are grateful for the financial support provided by the Australian Government Research Training Program (RTP) scholarship.

## References

- Bolton, M. D., M. W. Gui, and R. Phillips. "Review of Miniature Soil Probes for Model Tests." In Proceedings of the 11th Southeast Asian Geotechnical Conference, pp. 85-90. 1993.
- Ciantia, M. O., Arroyo, M., Butlanska, J., & Gens, A. (2016). "DEM modelling of cone penetration tests in a double-porosity crushable granular material". *Computers and Structures*, 73, 109-127. <http://dx.doi.org/10.1016/j.compgeo.2015.12.001>
- Giretti, D., K. Been, V. Fioravante, and S. Dickenson. "CPT Calibration and Analysis for a Carbonate Sand." *Géotechnique* 68, no. 4: 345-57. 2018. <https://doi.org/10.1680/jgeot.16.P.312>
- Idriss, I. M., and R. W. Boulanger. "Soil Liquefaction During Earthquakes." *Earthquake Engineering Research Institute*, 2008.
- Jamiolkowski, M., D. C. Lo Presti, and M. Manassero. "Evaluation of Relative Density and Shear Strength of Sands from CPT and DMT." In *Geotechnical Special Publication*, 119:201-38. New York, NY: American Society of Civil Engineers, 2003. [https://doi.org/10.1061/40659\(2003\)7](https://doi.org/10.1061/40659(2003)7)
- Lehane, B. M., V. Zania, S. H. Chow, and M. Jensen. "Interpretation of Centrifuge CPT Data in Normally Consolidated Silica and Carbonate Sands." *Géotechnique* 73, no. 10: 907-16. 2023. <https://doi.org/10.1680/jgeot.21.00177>
- Liao, S. S. C., and R. V. Whitman. "Overburden Correction Factors for SPT in Sand." *Journal of Geotechnical Engineering* 112, no. 3: 373-77. 1986. [https://doi.org/10.1061/\(ASCE\)0733-9410\(1986\)112:3\(373\)](https://doi.org/10.1061/(ASCE)0733-9410(1986)112:3(373))
- Liu, Q. B., and B. M. Lehane. "The Influence of Particle Shape on the (Centrifuge) Cone Penetration Test (CPT) End Resistance in Uniformly Graded Granular Soils." *Géotechnique* 62, no. 11: 973-84. 2012. <https://doi.org/10.1680/geot.10.P.077>
- Lunne, T., and H. P. Christoffersen. "Interpretation of Cone Penetrometer Data for Offshore Sands." In *Offshore Technology Conference*, pp. OTC-4464. OTC, 1983.
- Miura, K., K. Maeda, M. Furukawa, and S. Toki. "Mechanical Characteristics of Sands with Different Primary Properties." *Soils and Foundations* 38, no. 4: 159-72. 1998. [https://doi.org/10.3208/sandf.38.4\\_159](https://doi.org/10.3208/sandf.38.4_159)

Mesri, Gholamreza, and Barames Vardhanabhuti. "Compression of Granular Materials." *Canadian Geotechnical Journal* 46, no. 4 (2009): 369–92. 2009. <https://doi.org/10.1139/T08-123>.

Salgado, R., and M. Prezzi. "Computation of Cavity Expansion Pressure and Penetration Resistance in Sands." *International Journal of Geomechanics* 7, no. 4: 251–65. 2007. [https://doi.org/10.1061/\(ASCE\)1532-3641\(2007\)7:4\(251\)](https://doi.org/10.1061/(ASCE)1532-3641(2007)7:4(251))

Santamarina, J. C., and G. C. Cho. "Soil Behaviour; the Role of Particle Shape." In *Advances in Geotechnical Engineering: The Skempton Conference - Proceedings of a Three-Day Conference on Advances in Geotechnical Engineering, Organised by the Institution of Civil Engineers*, 604–17. London: Thomas Telford, 2004.

Tian, Y., and B.M. Lehane. "Parameters Affecting the CPT Resistance of Reconstituted Sands." In *Cone Penetration Testing 2022*, 734–40. CRC Press, 2022. <https://doi.org/10.1201/9781003308829-108>

Robertson, P.K., and R.G. Campanella. "Interpretation of Cone Penetration Tests. Part I: Sand." *Canadian Geotechnical Journal* 20, no. 4: 718–33. 1983. <https://doi.org/10.1139/t83-078>

Sturm, A. P. "On the Liquefaction Potential of Gravelly Soils: Characterization, Triggering and Performance." ProQuest Dissertations Publishing. 2019.